Supplementary Information : Cross-Platform Comparison of Arbitrary Quantum Computations

S1 Greedy method in the regime $M_S \gg 2^N$

The parameters M_U and M_S can be optimized through minimizing the statistical error with grid search [1,2] or using the perform importance sampling with partial information on the quantum state [3]. Both approaches require prior knowledge or simulation of the target state. Here, we devise a greedy method for sampling the unitary operation U that reduces the statistical error without prior knowledge of the target state. The statistical error as a function of M_U converges faster than uniformly sampling the unitary operation when the number of shots $M_S \gg 2^N$, where N is the number of qubits. Therefore, the greedy method is particularly useful for 5- and 7-qubit experiments. In this section, we demonstrate the comparison between the greedy method and random method for 5-qubit GHZ state.

When performing the fidelity estimation using randomized measurement, there are two major source of errors, the shot noise error and the the error from the incomplete tomography. The shot noise error can be suppressed when the number of shots $M_S \gg 2^N$. In this section, we propose the greedy method for sampling the random unitary in order to mitigate the error from the incomplete tomography. Instead of uniformly sampling the random unitary from a set of unitary operators U, we generate a sequence of unitary operators while maximizing the distance between each random unitary. Specifically, we define the distance between two unitary

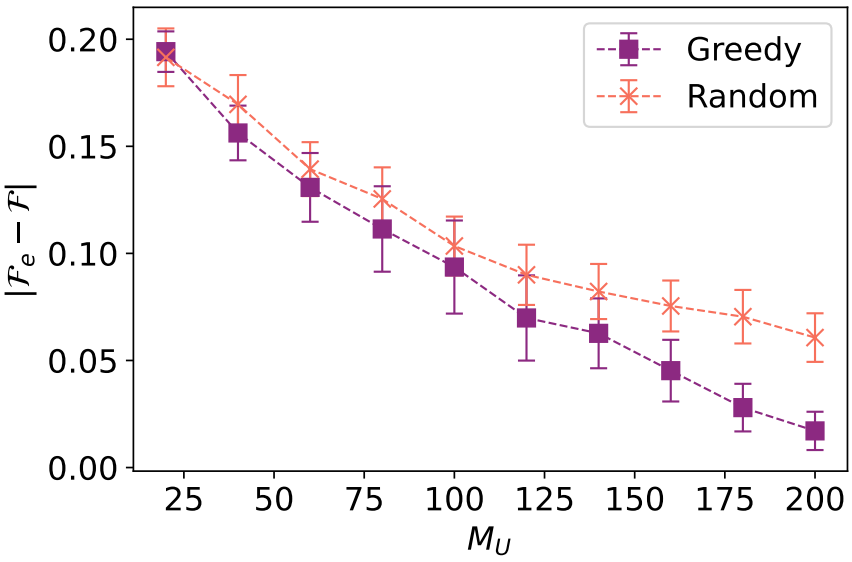

Figure S1: Comparison of error scaling for the fidelity of the GHZ states generated from UMD_1 vs IBM_1 with greedy or random sampling method for M_U.

operators as $d(u_a, u_b) = \max_\rho ||u_a \rho u_a^\dagger - u_b \rho u_b^\dagger)||_1$. And we generate the M_U unitary operators $\{u_i\}$, where $1 \leq i \leq M_U$ sequentially. For $i = 1$, we sample a unitary operator randomly from V. For $i > 1$, we search for a unitary operator u_i that minimizes the cost function $C(u_i; u_1, \ldots, u_{i-1}) = -\sum_{j=1}^{i-1} d(u_i, u_j)$. In order to minimize the cost function efficiently, we randomly generate N_{sample} distinct unitary operators $u_{i,x}$, where $1 \leq x \leq N_{\text{sample}}$ and we define $u_i = \min_{u_{i,x}} C(u_{i,x}; u_1, \ldots, u_{i-1})$. In practice, we find that $N_{\text{sample}} = 200$ is enough to find the minimum for $N = 7$ and $V = Cl(2)^{\otimes N}$, where $Cl(2)$ is the single qubit Clifford group. The greedy method is summarized in Algorithm 1.

Algorithm 1 Greedy method for sampling random unitary

Input : Number of random unitary M_U, a set of unitary operator S

Output : M_U random unitary operations for randomized measurement $\{u_i\}$, where $1 \leq i \leq M_U$.

1 : Sample u_1 randomly from S.

2 : **for** $i = 2$ **to** M_U **do**

3 : Find a unitary $u_i \in S$ to minimize the cost function $C(u_i; u_1, \ldots, u_{i-1})$.

4 : **end for**

5 : **return** $\{u_i\}$

We compare the two different methods of sampling the random unitary U: the randomized sampling and the greedy method. Using these two methods, we evaluate the fidelity between the state prepared on the UMD_1 system and that prepared on the IBM_1 system, by sampling subset of various size M_U from the full state tomography measurements. Fig. S1 shows the error of the fidelity estimation between UMD_1 and IBM_1 as function of M_U for $M_S = 2000$. We see that the greedy method outperforms the random method in this regime.

S2 Full state tomography vs. randomized measurement for 5-qubit GHZ state

Here, we compare the cross-platform fidelity obtained from full-state tomography and that from the randomized measurement on the 5-qubit GHZ state prepared on different platforms. We perform the full-state-tomography on a platform by measuring all the 243 independent 5-qubit Pauli operators. To do so, we first independently generate the 5-qubit GHZ state circuits on each plat-

form. Then we append different single-qubit rotations to the circuit to create the 243 different circuits. Each of the circuits gives the projective measurement result of one of the 243 independent 5-qubit Pauli operators. We set $M_S = 2000$ for all the platforms. For the randomized measurement, because a random Pauli basis measurement is equivalent to a randomize measurement with single qubit Clifford gate [2], we directly sample from the 243 Pauli basis measurements used for the full state tomography.

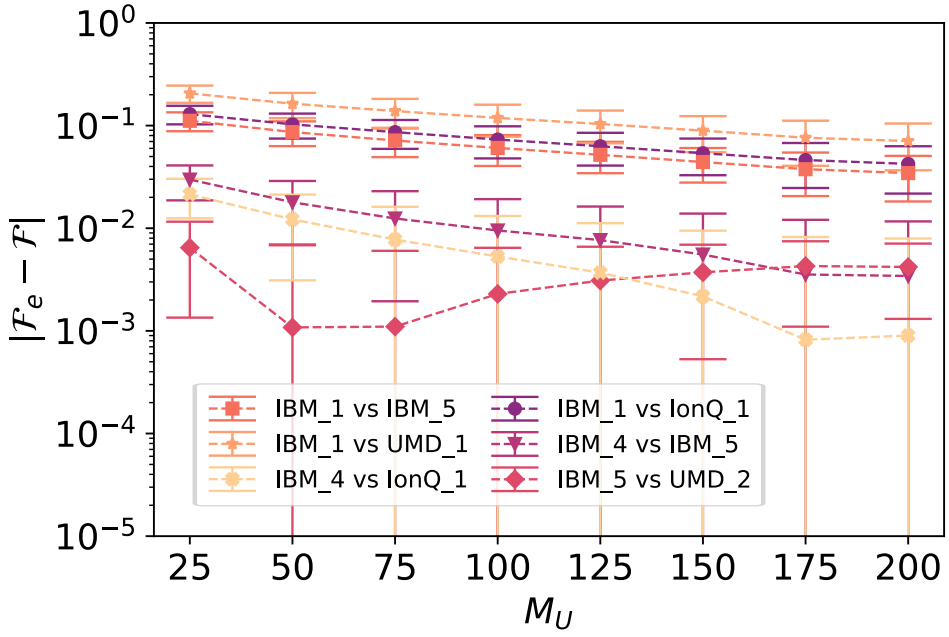

Figure S2: Fidelity error, $|\mathcal{F}_e - \mathcal{F}|$, for 6 randomly selected 5-qubit GHZ state cross-platform fidelities implemented on different platforms vs. number of randomized measurements M_U. The number of measurement is $M_S = 2000$ for all cases.

We calculate the cross-platform fidelity between as function of the number of randomized measurements M_U. The fidelity error $|\mathcal{F}_e - \mathcal{F}|$ is defined as the difference between the fidelity estimated by the randomized measurement $\mathcal{F}_e$ and the fidelity calculated through full state tomography

$\mathcal{F}$. The averaged error $|\mathcal{F}_e - \mathcal{F}|$ and the standard deviation are calculated through bootstrap resampling method [4]. The result (Fig. S2) shows that with only a fraction of the full state tomography measurements, one can estimate the cross-platform fidelity accurately.

S3 SWAP overhead for quantum volume circuit

Two-qubit gates on non-nearest-neighbor pairs are not directly available on superconducting quantum computers. To realize such non-nearest-neighbor two-qubit gates effectively, extra SWAP gates are necessary. Each SWAP gate consists of three CNOT gates, which cause non-trivial degradation to the overall fidelity of a circuit.

Optimizing the qubit routing can effectively decrease the number of involved non-nearest-neighbor two-qubit gates in evaluating the quantum volume circuits. But as the number of layers d increases, the number of non-nearest-neighbor two-qubit gates needed increases. In fig. S3 we show the mean value of two-qubit gates needed to implement quantum volume circuits of d layers on different platforms. As shown in the figure, the extra overhead grows linearly with d.

S4 Quantum systems

In this section we detail the quantum systems used in this study.

IBM Quantum Experience

We use IBM Quantum Experience service to access several of their superconducting quantum

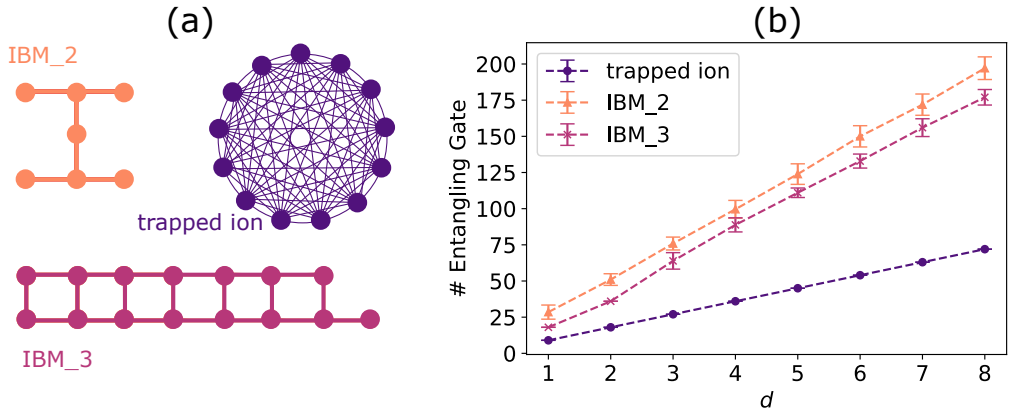

Figure S3: (a) Connectivity graph of IBM_2, IBM_3, and trapped ion (UMD_1 as an example) (b) Average number of two-qubit (entangling) gates needed to implement quantum volume circuits of layer d, on different quantum computers. The trapped ion quantum computers have the same all-to-all connectivity.

computers. [5] The ones used are *ibmq_belem* (IBM_1), *ibmq_casablanca* (IBM_2), *ibmq_melbourne* (IBM_3), *ibmq_quito* (IBM_4), and *ibmq_rome* (IBM_5). All the IBM systems use superconducting transmon qubits. The native gate sets are made of arbitrary single qubit rotations and nearest-neighbor two-qubit CNOT gates according to the connectivity graph. The error of single-qubit gates in IBM systems ranges from 3.32×10^{-4} to 5.03×10^{-2}, and the two-qubit errors range from 7.47×10^{-3} to 1.07×10^{-1}. Detailed specifications of each quantum device including qubit-connectivity diagram can be found on (https://quantum-computing.ibm.com/). On this platform, the synthesis and circuit optimization are implemented using the QISKit open-source software [6].

TI_EURIQA (UMD_1)

Error-corrected Universal Reconfigurable Ion-trap Quantum Archetype (EURIQA) is a trapped-

ion quantum computer currently located at the University of Maryland. This quantum computer supports up to thirteen qubits in a single chain of fifteen trapped $^{171}\mathrm{Yb}^{+}$ ions in a microfabricated chip trap [7]. The system achieves native single-qubit gate fidelities of 99.96% and two-qubit XX gate fidelities of 98.5-99.3%[8]. On this platform, we compile the circuits to its native gate set through KAK decomposition. We optimize the qubit assignment through exhaustive search to minimize the anticipated noise of entangling gates. No SPAM correction was applied in post-processing.

TI_UMD (UMD_2)

The second trapped-ion quantum computer system at Maryland is part of the TIQC (Trapped Ion Quantum Computation) team. This quantum computer supports up to nine qubits made of a single chain of $^{171}\mathrm{Yb}^{+}$ ions trapped in a linear Paul trap with blade electrodes [9]. Typical single- and two-qubit gate fidelities are $99.5(2)\%$ and $98-99\%$, respectively. On this platform, we compile the quantum volume to its native gate set through KAK decomposition. We apply SPAM correction to mitigate the detection noise assuming that the preparation noise is negligible.

IonQ (IonQ_1 and IonQ_2)

The commercial trapped-ion quantum systems used by IonQ contain eleven fully connected qubits in a single chain of $^{171}\mathrm{Yb}^{+}$ ions trapped in a linear Paul trap with surface electrodes [9]. The single-qubit fidelities are 99.7% for both systems at the time of measurement, while two-qubit fidelities are $95-96\%$ and $96-97\%$ for IonQ_1 and IonQ_2 respectively. On this platform, we

apply the technique describe in Ref. [10] to optimize the circuit. Quantum volume circuits were decomposed in terms of partially entangling MS gates. No SPAM correction was applied in post-processing.

1. Elben, A. *et al.* Cross-platform verification of intermediate scale quantum devices. *Phys. Rev. Lett.* **124**, 010504 (2020).

2. Huang, H.-Y., Kueng, R. & Preskill, J. Predicting many properties of a quantum system from very few measurements. *Nature Physics* **16**, 1050–1057 (2020).

3. Rath, A., van Bijnen, R., Elben, A., Zoller, P. & Vermersch, B. Importance sampling of randomized measurements for probing entanglement. *arXiv preprint arXiv:2102.13524* (2021).

4. Efron, B. & Gong, G. A leisurely look at the bootstrap, the jackknife, and cross-validation. *The American Statistician* **37**, 36–48 (1983).

5. Ibm quantum. https://quantum-computing.ibm.com/, 2021 .

6. Cross, A. The ibm q experience and qiskit open-source quantum computing software. In *APS March Meeting Abstracts*, vol. 2018, L58–003 (2018).

7. Maunz, P. L. W. High optical access trap 2.0. (2016).

8. Egan, L. *et al.* Fault-tolerant operation of a quantum error-correction code. *arXiv preprint arXiv:2009.11482* (2020).

9. Debnath, S. *et al.* Demonstration of a small programmable quantum computer with atomic qubits. *Nature* **536**, 63–66 (2016).

10. Nam, Y., Ross, N. J., Su, Y., Childs, A. M. & Maslov, D. Automated optimization of large quantum circuits with continuous parameters. *npj Quantum Information* **4**, 1–12 (2018).